Inorganic Chemistry

Article

pubs.acs.org/IC

Tetraalkylammonium Uranyl Isothiocyanates

Clare E. Rowland,[†,‡] Mercouri G. Kanatzidis,[†,§] and L. Soderholm*[,‡]

[†]Department of Chemistry, Northwestern University, 2145 Sheridan Road, Evanston, Illinois 60208, United States

[‡]Chemical Sciences and Engineering Division and [§]Materials Science Division, Argonne National Laboratory, Argonne, Illinois 60439, United States

Supporting Information

ABSTRACT: Three tetraalkylammonium uranyl isothiocyanates, $[(CH_3)_4N]_3UO_2(NCS)_5$ (**1**), $[(C_2H_5)_4N]_3UO_2(NCS)_5$ (**2**), and $[(C_3H_7)_4N]_3UO_2(NCS)_5$ (**3**), have been synthesized from aqueous solution and their structures determined by single-crystal X-ray diffraction. All of the compounds consist of the uranyl cation equatorially coordinated to five N-bound thiocyanate ligands, $UO_2(NCS)_5^{3-}$, and charge-balanced by three tetraalkylammonium cations. Raman spectroscopy data have been collected on compounds **1**−**3**, as well as on solutions of uranyl nitrate with increasing levels of sodium thiocyanate. By tracking the Raman signatures of thiocyanate, the presence of both free and bound thiocyanate is confirmed in solution. The shift in the Raman signal of the uranyl symmetric stretching mode suggests the formation of higher-order uranyl thiocyanate complexes in solution, while the solid-state Raman data support homoleptic isothiocyanate coordination about the uranyl cation. Presented here are the syntheses and crystal structures of **1**−**3**, pertinent Raman spectra, and a discussion regarding the relationship of these isothiocyanates to previously described uranyl halide phases, $UO_2X_4^{2-}$.

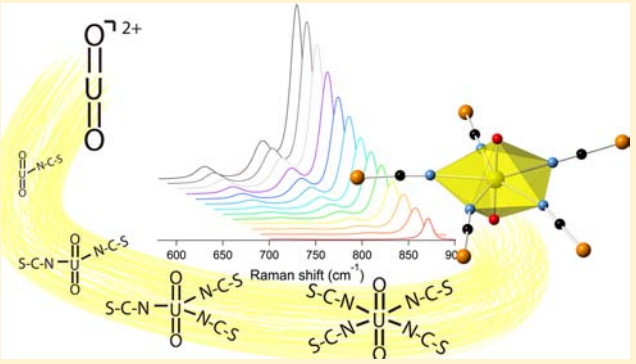

INTRODUCTION

Structural details concerning the interaction of thiocyanate (SCN^-) with cationic lanthanides and actinides may provide insight into the mechanistic role played by the anion in enhancing 4f−5f separations using solvent extraction techniques.[1−3] Inherently difficult to affect because of their similar chemistries, lanthanide−actinide separations have become a recent area of interest as advanced systems are considered for nuclear energy production.[4] These systems require separation of the heavier actinides, which can be recycled, from their lanthanide counterparts, which strongly absorb neutrons and thus inhibit material reuse. Liquid−liquid extraction techniques are the current separation method of choice. They rely on small free-energy differences between complexes of the targeted metal ion in two immiscible solutions. Generally, the f ion is extracted from an aqueous phase containing the mixture into an organic, nonpolar phase, from which the targeted species is then isolated. Energy differences driving these separations are small; for example, at 25 °C an increased stabilization energy of 1.4 kcal/mol for the metal in the organic phase results in an increase in the separation factor (concentration ratio in the two phases) by a factor of 10.

The addition of thiocyanate anion to a solvent extraction system has been reported to significantly enhance the ability to selectively move an actinide versus a lanthanide ion into the organic phase,[1−3] even outperforming other pseudohalides.[5,6] Suggested by these observations is an underlying structural difference between their coordination complexes in solution. Upon extraction as a thiocyanate anionic complex, the initial speculation focused on the possibility that subtle differences in hardness of the 4f versus 5f ions underpin an enhanced tendency of an actinide over a lanthanide to form inner-sphere complexes with thiocyanate.[1,6−11] The assumption underlying this explanation is that such differences in coordination would be sufficient to impact separations. Our recent studies using high-energy X-ray scattering to correlate complexant structures in solution with experimentally obtained stability constants do not support this argument but are instead consistent with previous suggestions that liquid−liquid separations cannot necessarily distinguish inner- versus outer-sphere ligand coordination.[12−14] Thus, we are left with no clear understanding of the underlying mechanism responsible for enhanced actinide separation in the presence of thiocyanate.

Although the focused interest and fundamental challenge rest in the separation of trivalent lanthanides from the heavier, trivalent actinides, the observations regarding thiocyanate interactions with f ions point to its potential as a system in which to probe subtle bonding differences between the 4f and 5f orbitals.[1,15−17] With this goal in mind, we have begun a broad study of the interaction of thiocyanate with a variety of f ions in an effort to distinguish the roles of electrostatics and bonding on the energetics of the complexes formed. Reported here are the initial findings on the interactions of uranyl with

Received: August 7, 2012
Published: October 16, 2012

   dx.doi.org/10.1021/ic301741u | *Inorg. Chem.* 2012, 51, 11798−11804

the thiocyanate anion, both in solution, as measured by Raman spectroscopy, and in the solid state, as quantified by single-crystal structure determinations for tetraalkylammonium salts of relevance to the solvent extraction process of interest.

EXPERIMENTAL SECTION

Synthesis. Compounds **1**−**3** were synthesized by combining solutions of uranyl nitrate, sodium thiocyanate, and tetraalkylammonium chloride salts in the amounts indicated in Table 1.

Table 1. Synthesis Details for 1−3

compound	$UO_2(NO_3)_2$ (1 M)	NaSCN (15 M)	counterion
$[(CH_3)_4N]_3UO_2(NCS)_5$ (**1**)	100 μL	66 μL	$[(CH_3)_4N]Cl$ (4 M); 200 μL
$[(C_2H_5)_4N]_3UO_2(NCS)_5$ (**2**)	100 μL	66 μL	$[(C_2H_5)_4N]Cl$ (2 M); 400 μL
$[(C_3H_7)_4N]_3UO_2(NCS)_5$ (**3**)	100 μL	66 μL	$[(C_3H_7)_4N]Cl$ (1 M); 800 μL

Tetrabutylammonium salts have quite poor solubility in water, which is why the investigation was terminated at tetrapropylammonium. The use of alternate solvents (e.g., methanol/water mixture) was considered in the interest of exploring the longer-chained tetraalkylammonium salts but ultimately not undertaken because our interest is focused specifically on the behavior of these compounds in water. During selection of the starting materials, it proved necessary to consider both potentially interfering ions and choices that were found to work. The nitrate in the uranyl nitrate starting material was undesirable because of its potential complexation with uranyl in solution or in the solid state, but the reactivity of thiocyanate toward acid precluded using a synthetic approach that involved the dissolution of UO_3 in HCl, for example. Although nitrate did not complex uranyl under the experimental conditions employed herein, chloride salts were chosen instead in order to optimize the probability of preparing homoleptic thiocyanate complexes. If chloride were to have been problematic, the direct reaction with tetraalkylammonium thiocyanate was considered as an alternative, but this option proved unnecessary.

The yellow uranyl nitrate solution turned orange upon the addition of thiocyanate, and a yellow precipitate formed immediately upon the addition of the tetraalkylammonium salt. The precipitate was a crystalline powder, as confirmed by powder X-ray diffraction, and contained a significant amount of NaCl (see the Supporting Information, S1−S3). Allowing the precipitate to remain in the mother liquor, open to the atmosphere to permit evaporation, yielded single crystals of **1** or of **2** and **3** over the course of several hours or several days, respectively. In order to isolate the target compounds in pure form, the precipitates were dissolved in acetone, in which the NaCl impurity was insoluble. Recrystallization from acetone yielded pure **1**−**3**, as confirmed by powder X-ray diffraction (Supporting Information, S4−S6). The yields of the products based on uranium were calculated as 93% (**1**), 92% (**2**), and 80% (**3**).

X-ray Structure Determination. Single crystals were isolated from the bulk and mounted on a Mitegen Micromount loop for data collection. Reflections were collected from 0.3° ω scans on a Bruker SMART diffractometer with an APEXII CCD detector using Mo Kα radiation. The data were integrated and an absorption correction was applied using the *APEXII* software suite.[18,19] The structure was solved by direct methods using *SHELXS-97* and refined using *SHELXL-97*.[20] Compound **2** was originally refined in a half-cell in space group *Pnma* with substantial disorder in the tetraethylammonium ions; however, collection of a better data set gave evidence for a doubled cell. Refining this compound in $P2_1/n$ not only yielded much improved R values but also eliminated the disorder that was observed in the smaller cell. Hydrogen atoms for all compounds were placed in calculated positions. Crystals of **3** were notably poorly diffracting, with this being the case with crystals both prepared as described in the Experimental Section and prepared at varied molar ratios. Ultimately, the most strongly diffracting of a large number of screened crystals was selected for data collection. Positional disorder on some carbon sites of the tetrapropylammonium cation in **3** was modeled using a PART command and refining the occupancy of the disordered sites to a total

Table 2. Summary of Crystallographic and Structural Refinement Data of 1−3

	1	**2**	**3**
formula	$[(CH_3)_4N]_3UO_2(NCS)_5$	$[(C_2H_5)_4N]_3UO_2(NCS)_5$	$[(C_3H_7)_4N]_3UO_2(NCS)_5$
empirical formula	$C_{17}H_{36}N_8O_2S_5U$	$C_{29}H_{60}N_8O_2S_5U$	$C_{41}H_{84}N_8O_2S_5U$
fw	782.87	951.23	1119.49
temp (K)	100	100	100
λ(Mo Kα)	0.71073	0.71073	0.71073
color	yellow	yellow	yellow
habit	block	block	block
cryst syst	monoclinic	monoclinic	monoclinic
space group	$P2_1/c$	$P2_1/n$	$P2_1/n$
a (Å)	16.365(3)	20.581(3)	12.543(3)
b (Å)	9.2621(16)	20.318(3)	11.934(3)
c (Å)	20.346(3)	20.589(3)	36.154(7)
α (deg)	90	90	90
β (deg)	97.754(2)	101.603(2)	91.890(3)
γ (deg)	90	90	90
V (Å^3)	3055.6(9)	8433.7(19)	5408.7(19)
Z	4	8	4
reflns collected	43211	66260	61024
indep reflns	8817 [R_{int} = 0.0715]	15390 [R_{int} = 0.0770]	9841 [R_{int} = 0.1057]
GOF	1.027	1.030	1.025
final R indices [$I > 2\sigma(I)$][a]	R_{obs} = 0.0393, wR_{obs} = 0.0836	R_{obs} = 0.0431, wR_{obs} = 0.0888	R_{obs} = 0.0574, wR_{obs} = 0.1208
R indices [all data][a]	R_{all} = 0.0613, wR_{all} = 0.0926	R_{all} = 0.0621, wR_{all} = 0.0974	R_{all} = 0.0977, wR_{all} = 0.1375
largest diff peak, hole (e/Å^3)	1.872, −1.484	1.535, −0.731	2.100, −0.962

[a] $R = \sum||F_o| - |F_c||/\sum|F_o|$, $wR = \{\sum[w(|F_o|^2 - |F_c|^2)^2]/\sum[w(|F_o|^4)]\}^{1/2}$ and calculated $w = 1/[\sigma^2(F_o^2) + (0.0675P)^2 + 1.4512P]$, where $P = (F_o^2 + 2F_c^2)/3$.

dx.doi.org/10.1021/ic301741u | *Inorg. Chem.* 2012, 51, 11798−11804

fixed at 100%. The final refinement resulted in an alkyl chain (C69A–C71A) that was 54% occupied and directly adjacent to the alkyl chain that accounted for the remainder of the electron density (C69B–C71B). A SAME command was used to constrain the bond lengths and angles of the other alkyl chains on the same cation. Crystallographic and structural refinement data are summarized in Table 2.

Powder X-ray diffraction data were collected on a Scintag X1 diffractometer (Cu Kα, 3–40°) to confirm the phase purity by comparison of experimental powder diffraction data with powder patterns calculated from the single-crystal structure determination.

Raman Spectroscopy. Raman spectra were collected on crushed single crystals of **1**–**3** as well as on aqueous solutions of uranyl nitrate with increasing concentration of sodium thiocyanate. Solutions were prepared by combining 1 *m* $UO_2(NO_3)_2$, 15 *m* NaSCN, and sufficient water to obtain final concentrations of 0.4 *m* UO_2^{2+} and 0, 0.4, 0.8, 1.2, 1.6, 2, 2.4, 3.2, 4, 4.8, 5.6, 6.4, and 7.2 *m* SCN^-. Spectra were collected on a Renishaw InVia Raman microscope using an excitation wavelength of 532 nm. A circular polarizer was used during the collection of spectra on solids; a normal polarizer was used on solutions. Solid samples were measured on a glass slide, while solution samples were contained in a quartz cuvette for measurement.

RESULTS AND DISCUSSION

Crystal Structures. Compounds **1**–**3** each consist of anionic uranyl isothiocyanate molecules and tetraalkylammonium counterions. The uranyl geometry is a pentagonal bipyramid, the apices of which are formed by the uranyl oxygen atoms; five equatorial positions are occupied by N-coordinated isothiocyanates, In all reported compounds, three tetraalkylammonium cations charge-balance each $UO_2(NCS)_5^{3-}$ unit. The packing of **1**–**3** down [010] are shown in Figure 1. Important interatomic distances and angles are summarized in Table 3. Thermal ellipsoid plots are available in the Supporting Information (S7–S9).

Although these compounds were synthesized from aqueous solution, there is no evidence of water in any of the structures, either coordinated to the uranyl cation or as a solvent in the crystal lattice. Metal thiocyanate compounds are typically synthesized in nonaqueous (and occasionally strictly anhydrous) media perhaps because of the higher solubility of larger tetraalkylammonium cations in small-chain alcohols rather than an expressed intent to exclude water from the product.[21,22]

That all of the thiocyanate ligands are coordinated to the uranyl cation by nitrogen linkages indicates the preference of the uranyl cation, a Lewis acid, to interact with the harder end of the ambidentate ligand. This manifestation of hard–soft acid–base chemistry is consistent with previously reported thiocyanate compounds, in which only very soft cations, such as Ba^{2+} and Ag^+, exhibit coordination to sulfur.[23,24] The uranyl moeity, with its formally divalent charge, should be softer than the trivalent and higher-valent lanthanides and actinides. Consequently, the absence of evidence for sulfur binding to the uranyl in the solid state is not unexpected and suggests that a similar mode of ligation may be expected in solution. Upon extrapolation to even harder f ions, which by analogy should all bind as hard Lewis acids, these results suggest that it is not a difference in binding of this ambidentate ligand that is responsible for its ability to distinguish the softer actinides from their harder 4f counterparts.

The 5-fold coordination geometry that the anion adopts about the uranyl cation is consistent with the prevalence of a pentagonal-bipyramidal coordination geometry in uranyl chemistry and, more specifically, with previously reported uranyl isothiocyanates. The $UO_2(NCS)_5^{3-}$ anion dominates the

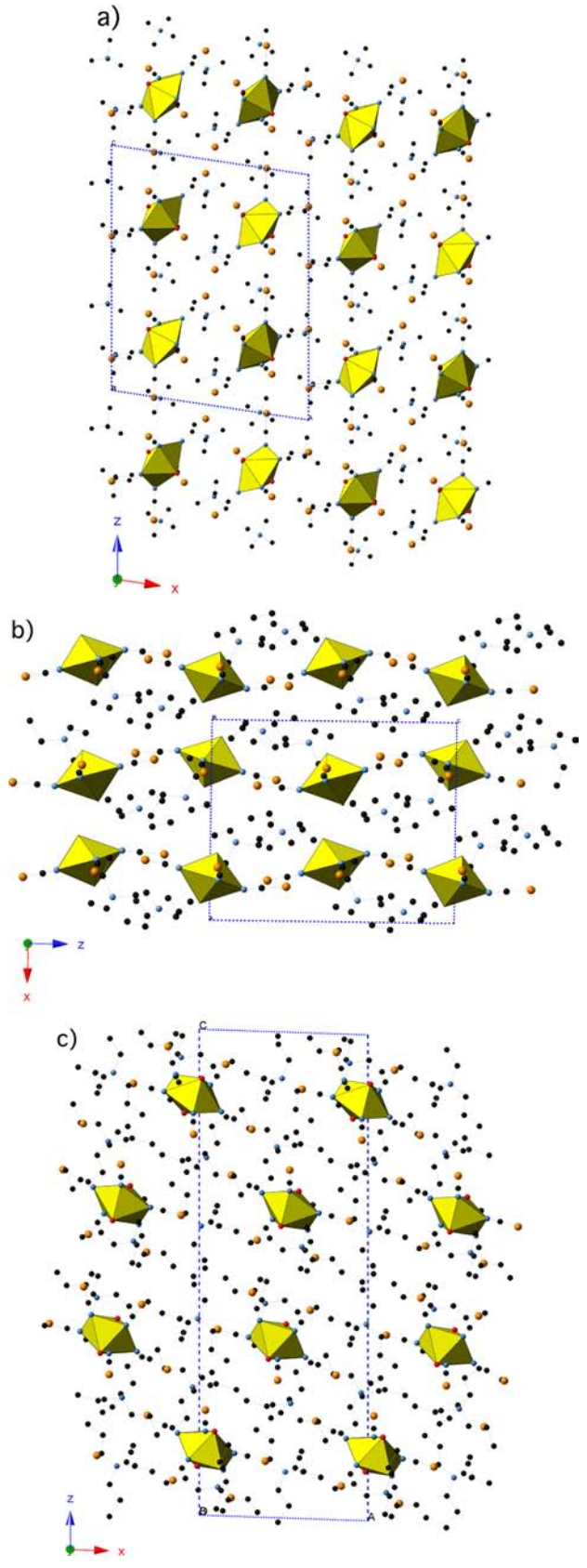

Figure 1. (a) View down [010] of **1**. Polyhedra are formed from the uranyl oxygen atoms (apices) and five nitrogen atoms about the uranyl cation. The unit cell is outlined in blue. (b) View down [010] of **2**. (c) View down [010] of **3**.

dx.doi.org/10.1021/ic301741u | *Inorg. Chem.* 2012, 51, 11798–11804

Table 3. Important Interatomic Distances and Angles

	1	2	3
U═O (Å)	1.773(3)	1.759(6)	1.747(5)
	1.768(3)	1.767(6)	1.752(6)
		1.772(7)	
		1.762(7)	
O═U═O (deg)	179.67(15)	177.4(3)	178.9(3)
		178.3(4)	
U−N (Å)	2.426(4)	2.444(7)	2.466(7)
	2.478(4)	2.439(8)	2.419(8)
	2.462(4)	2.449(6)	2.449(7)
	2.436(4)	2.458(9)	2.435(7)
	2.440(4)	2.427(7)	2.408(8)
		2.464(8)	
		2.492(9)	
		2.423(7)	
		2.448(7)	
		2.438(8)	
N−N (Å)	2.845(6)	2.819(9)	2.845(11)
	2.911(6)	2.826(9)	2.904(10)
	2.842(6)	2.828(10)	2.853(10)
	2.885(6)	2.833(10)	2.934(11)
	2.927(6)	2.835(10)	2.787(10)
		2.855(10)	
		2.916(9)	
		2.946(10)	
		2.949(10)	
		2.989(10)	
N−N−N−N (deg)	0.4(2)	0.2(4)	0.1(4)
	7.3(2)	1.1(4)	5.0(4)
	8.0(2)	1.2(4)	4.9(4)
	12.4(2)	2.8(4)	7.9(4)
	12.6(2)	2.9(4)	7.9(4)
		3.0(4)	
		3.5(4)	
		3.6(4)	
		5.0(4)	
		5.4(4)	
average U═O (Å)	1.770(4)	1.763(6)	1.749(4)
average U−N (Å)	2.45(2)	2.45(2)	2.44(2)
average N−N (Å)	2.88(4)	2.88(6)	2.86 (6)

structural literature, stabilized with a variety of counterions, including alkali metals,[25−27] ammonium,[25] pyridinium-based cations,[28] and others.[29] Even when thiocyanate fails to fill the inner coordination sphere of the uranyl cation, pentagonal bipyramids remain the prevalent coordination in uranyl thiocyanate structural chemistry.[21,30−40] In view of the classification of thiocyanate as a pseudohalide, 5-fold thiocyanate coordination is somewhat unexpected because uranyl halides typically exhibit square bipyramid coordination and thus 4-fold coordination by the halide.[41−43]

The archetypal uranyl tetrahalide moiety is prevalent in reported uranyl chloride and bromide structures.[44] Other compounds generally contain at least one nonhalide atom coordinated to the uranyl cation, and among these are found examples demonstrating a range of possible uranyl coordination geometries. Uranyl fluoride compounds differ notably from the heavier halides in that all homoleptic examples (about 20% of the reported structures)[44] exhibit pentagonal-bipyramidal geometry.

A closer examination of the tetra- and pentahalides reveals that the difference in coordination behavior between fluoride and the heavier halides may result in part from steric effects, notably electrostatic repulsion. As shown in Figure 2, the

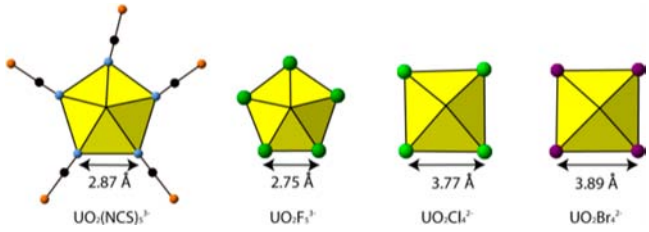

Figure 2. Average distance between thiocyanate nitrogen atoms about the uranyl cation in **1**−**3** compared to the average interhalide distances in uranyl pentafluoride, tetrachloride, and tetrabromide species. The N−N distance was averaged from values provided in Table 3, and the distances for the uranyl halides were taken from published literature.[44]

average distance between adjacent fluoride ions in the uranyl pentafluoride molecule, 2.75 Å, appears to be too short to accommodate chloride ions (radius 1.81 Å[45]) in the same geometry, even when factoring in the increased uranyl−halogen bond distances expected for chloride and bromide ions. By contrast, the thiocyanate anion exhibits N-coordination to the uranyl cation, thus easing steric constraints and permitting a fifth equatorial ligand; the resulting complex adopts pentagonal-bipyramidal geometry.[46] Likewise, other pseudohalides might be expected to coordinate through ions of relatively small ionic radius (e.g., cyanate, cyanide, N_3^-) to exhibit pentagonal-bipyramidal geometry, an expectation that is supported by the literature.[47−49] Finally, it is worth mentioning that although electrostatic repulsion between fluoride and thiocyanate anions is not sufficient to prevent 5-fold coordination about the uranyl cation, it may explain torsion that is observed in the equatorially bound species, particularly in **1**, and may also play a role in the slight distortion of the uranyl ion from a linear geometry, as shown in Table 3.

Raman Spectroscopy. Normalized Raman spectra, collected from crushed single crystals of **1**−**3**, are shown from 3200 to 300 cm^{-1} in Figure 3. The relevant spectral features and their assignments are summarized in Table 4; those not assigned are consistent with Raman spectra of the corresponding tetraalkylammonium salt (see the Supporting

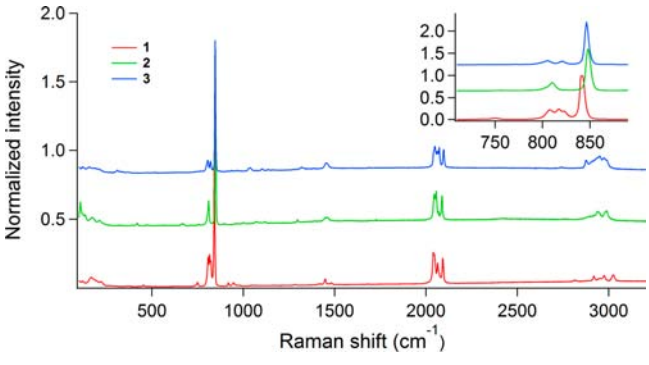

Figure 3. Raman spectra of single crystals of **1**−**3** shown from 3200 to 300 cm^{-1}. (inset) Raman spectra of single crystals of **1**−**3** shown from 900 to 700 cm^{-1}. $\nu_{sym}(UO_2^{2-})$ falls between 847 and 841 cm^{-1}. Also evident is ν(CS) associated with bound thiocyanate (around 810 cm^{-1}), while ν(CS) from free thiocyanate is notably absent.

dx.doi.org/10.1021/ic301741u | Inorg. Chem. 2012, 51, 11798−11804

Table 4. Features and Assignments of Raman Data

Raman shift in the solid state (cm^{-1})	Raman shift in solution (cm^{-1})	Raman shift in the literature (cm^{-1})	signal	reference
2090–2043 (**1**), 2088–2047 (**2**), 2098–2045 (**3**)	2072	2100–2050	ν(CN)	50
	1660	1641	ν_2(OH)	51
	1050	1050, 1048	$\nu_1(NO_3^-)$	52, 53
841 (**1**), 847 (**2**), 846 (**3**)	871–848[a]	871, 868	$\nu_{sym}(UO_2)$	53, 54
822–808 (**1**), 810 (**2**), 821–806 (**3**)	820–814	860–780	ν(CS) (bound)	50
	750	747	ν(CS) (free)	55

[a]Raman peak of the UO_2^{2+} aqua ion is observed at 871 cm^{-1}; the $\nu_{sym}(UO_2^{2+})$ peak shifts upon complexation with thiocyanate.

Information, S10–S12). The region from 900 to 700 cm^{-1}, enlarged as an inset to Figure 3, highlights the uranyl symmetric stretch, appearing at 847 cm^{-1} (**2**), 846 cm^{-1} (**3**), and 841 cm^{-1} (**1**). The shift to lower energy of the uranyl stretch may be expected to correlate with a weakening of the U–O bond, which would manifest itself structurally as a lengthening of the bond; however, this trend is not supported by the refined structural metrics provided in Table 3. Although the compound with the longest dioxo U–O (-yl) bond (**1**) may have the lowest-energy Raman shift, the relationship between bond length and Raman shift is reversed for the remaining two compounds. We note, however, the proximity of the Raman signals to each other relative to the resolution of the instrument (approximately 3 cm^{-1}) and that the U–O bond lengths do not differ by more than 3 standard deviations.

Visible in the Figure 3 inset is the C–S stretch near 810 cm^{-1} associated with bound thiocyanate. As expected, the C–S stretch corresponding to free thiocyanate, which would be expected at 750 cm^{-1}, is absent from these spectra. A small signal at 748 cm^{-1} in **1** can be attributed to tetramethylammonium in the compound (see the Supporting Information, S10).

Raman spectra are presented in Figure 4 from uranyl nitrate (0.4 *m*) solutions with increasing concentrations of sodium thiocyanate (0–7.2 *m*). The data have been normalized to the intensity of the nitrate peak at 1050 cm^{-1}. Assignments of the spectral features are also summarized in Table 4. It should be noted that the symmetric stretch of the free nitrate ion (ν_1) is expected at 1050 cm^{-1}, whereas a coordinated nitrate group may be seen anywhere between 1050 and 1000 cm^{-1}.[52] In the case of uranyl nitrate specifically, bound nitrate is observed at 1036 cm^{-1};[53] therefore, we have attributed the signal at 1050 cm^{-1} strictly to free nitrate. This assignment also agrees with previously published data indicating that bound nitrate is not detected in uranyl nitrate solutions with concentrations below 1.5 M.[53] Although determined under markedly different solution conditions than those present in our system, a relatively low stability constant for the formation of the first nitrate complex with the uranyl cation ($\log \beta_1^\circ = 0.30 \pm 0.15$)[56] also supports our assignment of the 1050 cm^{-1} Raman peak to free nitrate.

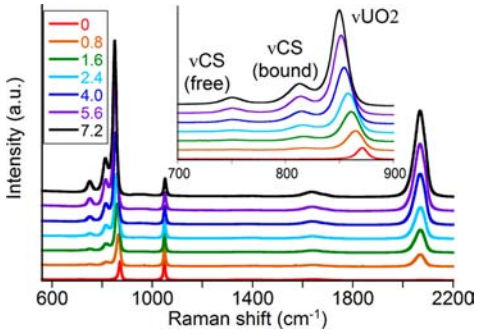

Figure 4. Normalized Raman spectra of uranyl nitrate solutions with increasing levels of sodium thiocyanate. Peak assignments are summarized in Table 4. (inset) Normalized spectra of uranyl nitrate and sodium thiocyanate solutions are shown from 900 to 725 cm^{-1}.

In the inset of Figure 4, normalized data are shown from 900 to 700 cm^{-1}, the region in which thiocyanate coordination to the uranyl cation can best be monitored. The peak at 750 cm^{-1} is observed in the spectrum obtained from a NaSCN solution (see the Supporting Information, S10–12) and corresponds to ν(CS) of uncoordinated thiocyanate.[50] A second peak, which develops in the presence of both uranyl and thiocyanate ions, appears from 814 to 820 cm^{-1} and is consistent with a CS stretching frequency of thiocyanate coordinated to a metal via a nitrogen linkage.[50] Both the free and bound thiocyanate peaks grow upon the addition of thiocyanate to the uranyl solution, indicating a distribution between solvent- and uranyl-bound complexes consistent with an equilibrium between free and bound thiocyanate. Both species are evident at the uranyl-to-thiocyanate ratio of 1:10 (0.4 *m* UO_2^{2+} and 4.0 *m* NaSCN), which corresponds to the relative concentrations in the solutions from which crystals were grown.

The apparent growth and shift of the third peak from 871 to 848 cm^{-1} is more complex. In the spectrum that contains no thiocyanate, this peak, at 867 cm^{-1}, is assigned to the symmetric stretch of the bare, water-coordinated uranyl ion.[53,54] Upon the addition of thiocyanate, the signal appears to shift to a lower wavenumber, which would correspond to destabilization of the uranyl–oxo bond, as expected upon complexation.[57] This is consistent with the appearance of $\nu(UO_2)$ around 845 cm^{-1} in the crystals of **1**–**3**, wherein the uranyl cation exhibits homoleptic thiocyanate ligation. Thus, as thiocyanate is added to the system, the uranyl cation sees an increase in the presence of the thiocyanate ion in its coordination environment, and as a result, its symmetric stretching frequency shifts to a lower wavenumber. Each uranyl thiocyanate moeity should have a uniquely destabilized uranyl cation and therefore a different uranyl symmetric stretching frequency. Moreover, just as the molar intensity of ν(CS) in free and bound thiocyanate differs, so too will the molar intensity of $\nu(UO_2)$ in each of these uranyl thiocyanate complexes. Thus, the apparent increase in the intensity of $\nu(UO_2)$ is independent of an increase in the concentration of the uranyl cation but rather is related to the changing molar intensity as uranyl thiocyanate speciation changes in solution.

Previously published Raman data obtained from tetraalkylammonium uranyl chloride and bromide compounds provide a comparison to the thiocyanate data presented herein. The published data indicate that a Raman peak at 840 cm^{-1} corresponds to the uranyl symmetric stretch in a solid tetraethylammonium uranyl chloride salt, whereas the same

dx.doi.org/10.1021/ic301741u | Inorg. Chem. 2012, 51, 11798–11804

feature seen from tetramethylammonium uranyl bromide occurs at 832 cm^{-1}.[58] Both are seen to occur at lower wavenumbers than the corresponding thiocyanate compounds reported in this publication, implying destabilization of the uranyl bond in the halides relative to the thiocyanates. Assuming simple electrostatic interactions between the uranyl and its ligands, the finding that the U═O stretch occurs at higher energy in the thiocyanates than in the halide complexes is unexpected. Whereas five thiocyanates coordinate about the uranyl cation, only four are reported for the chloride and bromide compounds, so assuming similar electrostatic interactions for the anions and destabilization of the U═O bond with increasing equatorial-anion coordination, the trend seen here is counter to expectation.

Included in the published literature is the report of an increase in the Raman frequency of the uranyl stretch to 869 cm^{-1} upon dissolution of the uranyl halide salts in dilute hydrohalic acid, an effect consistent with displacement of the halide in the uranyl inner coordination sphere by water.[58] Such behavior would be consistent with thermodynamic expectations[56,59] and X-ray structural studies[14,43] of uranyl solution speciation. Although the concentration of the acid and therefore the free halide in solution is not reported, this Raman frequency is consistent with a slight shift from the hydrated uranyl peak, indicating that there has been some bound halide displaced by water. In the thiocyanate system, the uranyl symmetric stretch is observed at this same frequency in a 0.4 *m* thiocyanate medium or at a 1:1 molar ratio with uranium. In other words, uranyl halide or uranyl thiocyanate complex formation appears, based on the change in the Raman frequency from the hydrated uranyl cation, to take place to a small extent and to be similar both in dilute hydrohalic acid and in a solution with a 1:1 uranyl-to-thiocyanate ratio.

CONCLUSION

The crystal structures and Raman spectra of three new tetraalkylammonium uranyl isothiocyanates isolated from aqueous solution are reported. The compounds all exhibit 5-fold thiocyanate coordination about the uranyl cation, resulting in a $UO_2(NCS)_5^{3-}$ unit that is charge-balanced by tetramethyl- (**1**), tetraethyl- (**2**), and tetrapropylammonium (**3**) cations. Raman spectra of these compounds and of solutions similar to those from which the compounds were grown confirm structural studies showing that only bound thiocyanate is present in the solid state, whereas in solution, there is evidence of both free and bound thiocyanate. Moreover, a shift in the symmetric stretching frequency of the uranyl cation to lower energy as a function of the increased thiocyanate concentration confirms the ligation of thiocyanate in solution to form higher order uranyl thiocyanate complexes; the appearance of this signal at even lower energy in the solid products is consistent with homoleptic thiocyanate coordination about the uranyl cation.

ASSOCIATED CONTENT

Supporting Information

Powder X-ray diffraction data, ORTEP representations, and CIFs of **1**−**3** as well as supplemental Raman spectra. This material is available free of charge via the Internet at http://pubs.acs.org. CIFs may also be obtained free of charge from the Cambridge Structural Database via www.ccdc.cam.ac.uk/data_request/cif by referencing CCDC 875600−875602.

AUTHOR INFORMATION

Corresponding Author

*E-mail: LS@anl.gov.

Notes

The authors declare no competing financial interest.

ACKNOWLEDGMENTS

This work was performed at Argonne National Laboratory, operated by UChicagoArgonne LLC for the United States Department of Energy under Contract DE-AC02-06CH11357, and was supported by a DOE Office of Basic Energy Sciences, Chemical Sciences, the Heavy Elements Program. C.E.R. gratefully acknowledges support by the National Science Foundation through a Graduate Research Fellowship and from Grant DMR-1104965.

REFERENCES

(1) Khopkar, P. K.; Mathur, J. N. *J. Inorg. Nucl. Chem.* **1980**, *42*, 109−113.
(2) Moore, F. L. *Anal. Chem.* **1964**, *36*, 2158−2162.
(3) Chiarizia, R.; Danesi, P. R.; Scibona, G.; Magon, L. *J. Inorg. Nucl. Chem.* **1973**, *35*, 3595−3604.
(4) Roberto, J.; de la Rubia, T. D. *Basic research needs of advanced nuclear energy systems*; Office of Basic Energy Sciences, U.S. Department of Energy: Washington, DC, 2006.
(5) Borkowski, M.; Krejzler, J.; Siekierski, S. *Radiochim. Acta* **1994**, *65*, 99−103.
(6) Borkowski, M.; Lis, S.; Siekierski, S. *J. Alloys Compd.* **1998**, *275*−*277*, 754−758.
(7) Harmon, H. D.; Peterson, J. R.; McDowell, W. J.; Coleman, C. F. *J. Inorg. Nucl. Chem.* **1972**, *34*, 1381−1397.
(8) Khopkar, P. K.; Mathur, J. N. *J. Inorg. Nucl. Chem.* **1974**, *36*, 3819−3825.
(9) Choppin, G. R.; Graffeo, A. J. *Inorg. Chem.* **1965**, *4*, 1254−1257.
(10) Choppin, G. R.; Ketels, J. *J. Inorg. Nucl. Chem.* **1965**, *27*, 1335−1339.
(11) Musikas, C.; Cuillerdier, C.; Chachaty, C. *Inorg. Chem.* **1978**, *17*, 3610−3615.
(12) Soderholm, L.; Skanthakumar, S.; Neuefeind, J. *Anal. Bioanal. Chem.* **2005**, *383*, 48−55.
(13) Soderholm, L.; Skanthakumar, S.; Wilson, R. E. *J. Phys. Chem. A* **2009**, *113*, 6391−6397.
(14) Soderholm, L.; Skanthakumar, S.; Wilson, R. E. *J. Phys. Chem. A* **2011**, *115*, 4959−4967.
(15) Diamond, R. M.; Street, K.; Seaborg, G. T. *J. Am. Chem. Soc.* **1954**, *76*, 1461−1469.
(16) Jorgensen, C. K. *Isr. J. Chem.* **1980**, *19*, 174−192.
(17) Choppin, G. R. *J. Less Common Met.* **1983**, *93*, 323−330.
(18) *Bruker*, 2008.3-0 ed.; Bruker AXS: Madison, WI, 2008.
(19) Sheldrick, G. *APEXII*, 2008/1 ed.; University of Gottingen: Gottingen, Germany, 2008.
(20) Sheldrick, G. *Acta Crystallogr., Sect. A* **2008**, *64*, 112−122.
(21) Farmer, J. M.; Kautz, J. A.; Kwon, H. S.; Mullica, D. F. *J. Chem. Crystallogr.* **2000**, *30*, 301−309−309.
(22) Martin, J. L.; Thompson, L. C.; Radonovich, L. J.; Glick, M. D. *J. Am. Chem. Soc.* **1968**, *90*, 4493−4494.
(23) Lu, S.-F.; He, M.-Y.; Huang, J.-L. *J. Struct. Chem. (China)* **1982**, *1*, 71−76.
(24) Brodersen, K.; Hummel, H. U.; Boehm, K.; Procher, H. *Z. Naturforsch., B: Anorg. Chem., Org.. Chem.* **1985**, *33*, 347−351.
(25) Markov, V. P.; Traggerim, E. N.; Shul'gina, I. M. *Russ. J. Inorg. Chem.* **1964**, *9*, 305−308.
(26) Alcock, N. W.; Roberts, M. M.; Brown, D. *Acta Crystallogr., Sect. B* **1982**, *38*, 2870−2872.
(27) Arutyunyan, E. G.; Porai-Koshits, M. A. *Zh. Strukt. Khim.* **1966**, *7*, 393−398.

(28) Bombieri, G.; Forsellini, E.; Graziani, R.; Pappalardo, G. C. *Transition Met. Chem.* **1979**, *4*, 70−72.
(29) Bagnall, K. W. *Lanthanides and Actinides*; Butterworth: London, 1972; Vol. 7, pp 139−156.
(30) Rogers, R. D.; Zhang, J.; Campbell, D. T. *J. Alloys Compd.* **1998**, *271*−*273*, 133−138.
(31) Artem'eva, M. Y.; Mikhailov, Y. N.; Gorbunova, Y. E.; Serezhkina, L. B.; Serezhkin, V. N. *Zh. Neorg. Khim.* **2003**, *48*, 1470−1472.
(32) Akhmerkina, Z. V.; Dobrynin, A. B.; Litvinov, I. A.; Gorbunova, Y. E.; Mikhailov, Y. N.; Serezhkina, L. B.; Serezhkin, V. N. *Zh. Neorg. Khim.* **2004**, *49*, 1543.
(33) Artem'eva, M. Y.; Dolgushin, F. M.; Antipin, M. Y.; Serezhkina, L. B.; Serezhkin, V. N. *Z. Naturforsch.* **2004**, *49*, 419.
(34) Medrish, I. V.; Peresypkina, E. V.; Virovets, A. V.; Serezhkina, L. B. *Zh. Neorg. Khim.* **2008**, *53*, 1121−1126.
(35) Medrish, I. V.; Virovets, A. V.; Peresypkina, E. V.; Serezhkina, L. B. *Zh. Neorg. Khim.* **2008**, *53*, 1115−1120.
(36) Akhmerkina, Z. V.; Peresypkina, E. V.; Virovets, A. V.; Serezhkina, L. B. *Zh. Neorg. Khim.* **2008**, *53*, 1495−1499.
(37) Serezhkina, L. B.; Marukhnov, A. V.; Peresypkina, E. V.; Virovets, A. V.; Medrish, I. V.; Pushkin, D. V. *Zh. Neorg. Khim.* **2008**, *53*, 907−911.
(38) Akhmerkina, Z. V.; Mikhailov, Y. N.; Gorbunova, Y. E.; Churakov, A. V.; Serezhkina, L. B.; Serezhkin, V. N. *Zh. Neorg. Khim.* **2005**, *50*, 1430−1435.
(39) Mikhailov, Y. N.; Orlova, I. M.; Shchelokov, R. N.; Gorbunova, Y. E.; Akhmerkina, Z. V.; Serezhkina, L. B.; Serezhkin, V. N. *Zh. Neorg. Khim.* **2006**, *51*, 451−455.
(40) Akhmerkina, Z. V.; Virovets, A. V.; Peresypkina, E. V.; Serezhkina, L. B. *Zh. Neorg. Khim.* **2006**, *51*, 271−276.
(41) Deifel, N. P.; Cahill, C. L. *CrystEngComm* **2009**, *11*, 2739−2744.
(42) Deifel, N. P.; Cahill, C. L. *C. R. Chim.* **2010**, *13*, 747−754.
(43) Wilson, R. E.; Skanthakumar, S.; Cahill, C. L.; Soderholm, L. *Inorg. Chem.* **2011**, *50*, 10748−10754.
(44) Allen, F. H. *Acta Crystallogr., Sect. B* **2002**, *58*, 380−389.
(45) *Tables of physical and chemical constants*, 16th ed.; Kaye and Laby Online at www.kayelaby.npl.co.uk, 1995.
(46) In *J. Chem. Phys.* **1956**, *25*, 1069, prevalance of the three SCN^- resonance structures is calculated. The form with a formal charge of zero on the nitrogen atom accounts for approximately 71%, with N^- accounting for 12% and N^{2-} for 17%. Even when the ionic radius based on these ratios is overestimated by using the radius for N^{3-} in place of N^- and N^{2-}, the effective ionic radius of the nitrogen atom in SCN^- is less than 1 Å, well below that of F^-.
(47) Sonnenberg, J. L.; Hay, P. J.; Martin, R. L.; Bursten, B. E. *Inorg. Chem.* **2005**, *44*, 2255−2262.
(48) Berthet, J.-C.; Thuery, P.; Ephritikhine, M. *Chem. Commun.* **2007**, 604−606.
(49) Charpin, P.; Lance, M.; Nierlich, M.; Vigner, D.; Livet, J.; Musikas, C. *Acta Crystallogr., Sect. C* **1986**, *42*, 1691−1694.
(50) Nakamoto, K. *Infrared and Raman spectra of inorganic and coordination compounds. Part b: Applications in coordination, organometallic, and bioinorganic chemistry*, 5th ed.; John Wiley & Sons, Inc.: New York, 1997.
(51) Carey, D. *J. Chem. Phys.* **1998**, *108*, 2669.
(52) Casellato, U.; Vigato, P. A.; Vidali, M. *Coord. Chem. Rev.* **1981**, *36*, 183−265.
(53) Brooker, M. H.; Huang, C. B.; Sylwestrowicz, J. *J. Inorg. Nucl. Chem.* **1980**, *42*, 1431−1440.
(54) Khulbe, P. K.; Agarwal, A.; Raghuvanshi, G. S.; Bist, H. D.; Hashimoto, H.; Kitagawa, T.; Little, T. S.; Durig, J. R. *J. Raman Spectrosc.* **1989**, *20*, 283−290.
(55) Strommen, D. P.; Plane, R. A. *J. Chem. Phys.* **1974**, *60*, 2643−2646.
(56) *Chemical thermodynamics of uranium*, 2nd ed.; Grenthe, I., Fuger, J., Konings, R. J. M., Lemire, R. J., Muller, A. B., Nguyen-Trung, C., Wanner, H., Eds.; Nuclear Energy Agency, Organisation for Economic Cooperation and Development: Paris, 2004.
(57) Nguyen Trung, C.; Begun, G. M.; Palmer, D. A. *Inorg. Chem.* **1992**, *31*, 5280−5287.
(58) Newbery, J. E. *Spectrochim. Acta, Part A* **1969**, *25*, 1699−1702.
(59) Awasthi, S. P.; Sundaresan, M. *Indian J. Chem.* **1981**, *20A*, 378−381.